

## Supporting Information for

### Nanogenerators Based on Vertically Aligned InN Nanowires

Guocheng Liu,<sup>\*a</sup> Songrui Zhao,<sup>b</sup> Robert D. E. Henderson,<sup>c</sup> Zoya Leonenko,<sup>c</sup> Eihab Abdel-Rahman,<sup>d</sup> Zetian Mi<sup>b</sup> and Dayan Ban<sup>\*a</sup>

<sup>a</sup> *Department of Electrical and Computer Engineering, Waterloo Institute for Nanotechnology, University of Waterloo, 200 University Ave. West, Waterloo, Ontario, N2L3G1, Canada*

<sup>b</sup> *Department of Electrical and Computer Engineering, McGill University, Montreal, Quebec, H3A 0E9, Canada*

<sup>c</sup> *Department of Physics & Astronomy, Waterloo Institute for Nanotechnology, University of Waterloo, Waterloo, Ontario, N2L 3G1, Canada*

<sup>d</sup> *Department of System Design Engineering, Waterloo Institute for Nanotechnology, University of Waterloo, Waterloo, Ontario, N2L 3G1, Canada*

\*g37liu@uwaterloo.ca

\*dban@uwaterloo.ca

#### Table of Contents

**Fig. S1:** Room-temperature Raman spectrum of Mg-doped InN NWs

**Fig. S2:** 3D positive and negative current output signals when scanning over an area of 10  $\mu\text{m} \times 10 \mu\text{m}$  for Si substrate, high-doped and low-doped GaN NWs

**Fig. S3:** Photograph of a fabricated *p*-type InN NWs-based nanogenerator.

**Fig. S4:** The capacitance-frequency response of InN NG device

**Fig. S5:** The schematic setup for measuring the output current/voltage of fabricated InN NW-based NGs.

**Fig. S6:** The piezoelectric characteristics of the NG devices

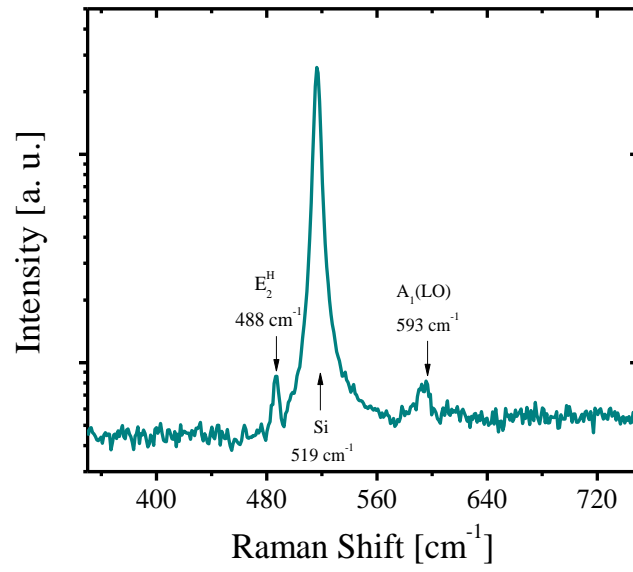
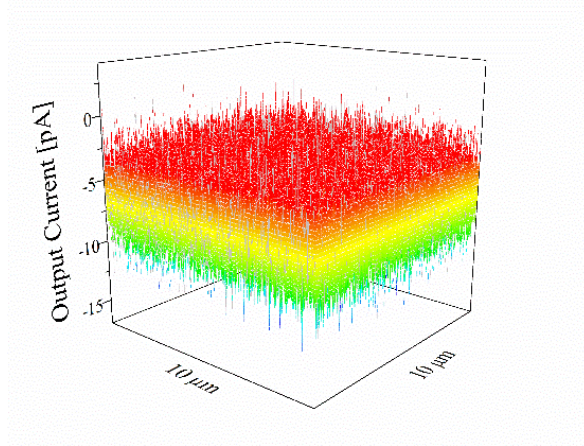
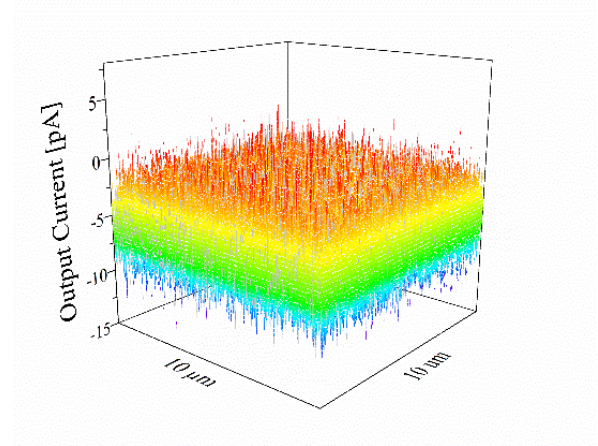


**Fig. S1** Room-temperature Raman spectrum of Mg-doped InN NWs, showing a very narrow E<sub>2</sub><sup>h</sup> phonon peak at 488 cm<sup>-1</sup> and A<sub>1</sub>(LO) mode at 593 cm<sup>-1</sup>.

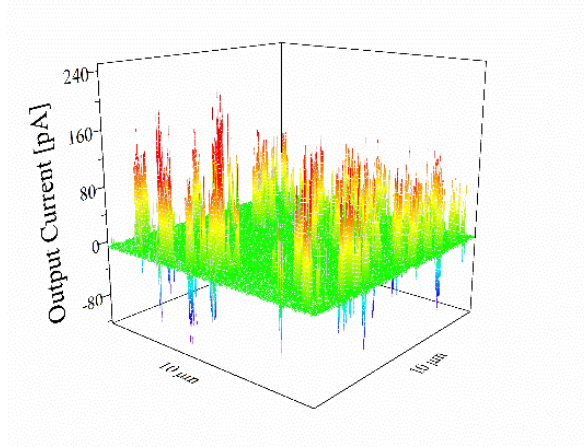
(a)



(b)



(c)



(d)

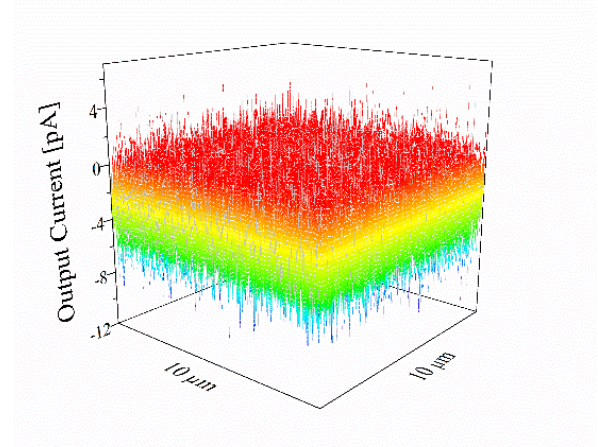


**Fig. S2** 3D positive and negative current output signals when scanning over an area of  $10\ \mu\text{m}\times 10\ \mu\text{m}$  for (a) Si substrate, (b) doped and (c) intrinsic GaN NWs with Pt tip and (d) *p*-type InN NWs with a Si tip.

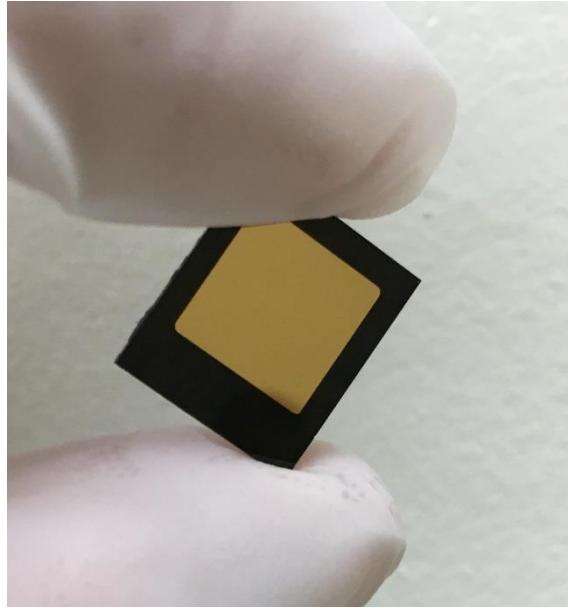


**Fig. S3** Photograph of a fabricated *p*-type InN NWs-based nanogenerator.

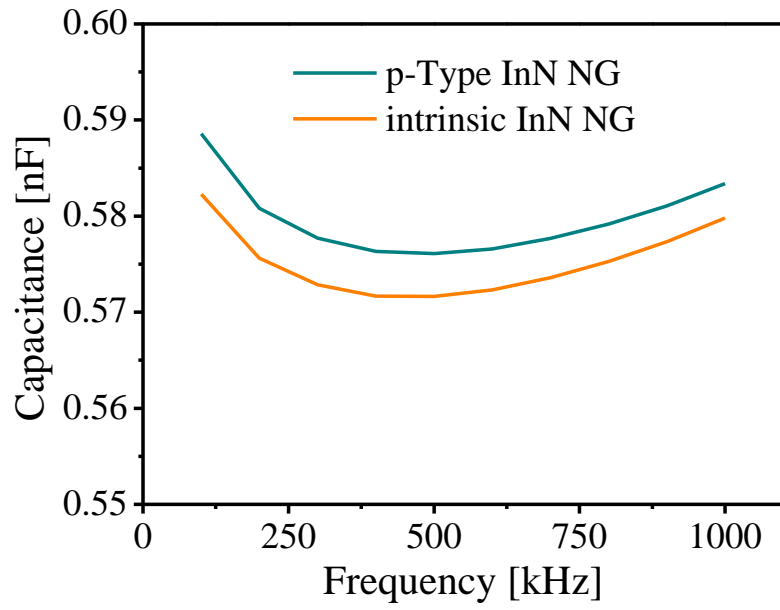


**Fig. S4** shows the capacitance-frequency response of InN NG device investigated by using Keithley 4200-SCS semiconductor characterization system that is carefully calibrated before measurements with the suppression of the noise down to 1fF in a wide frequency range.

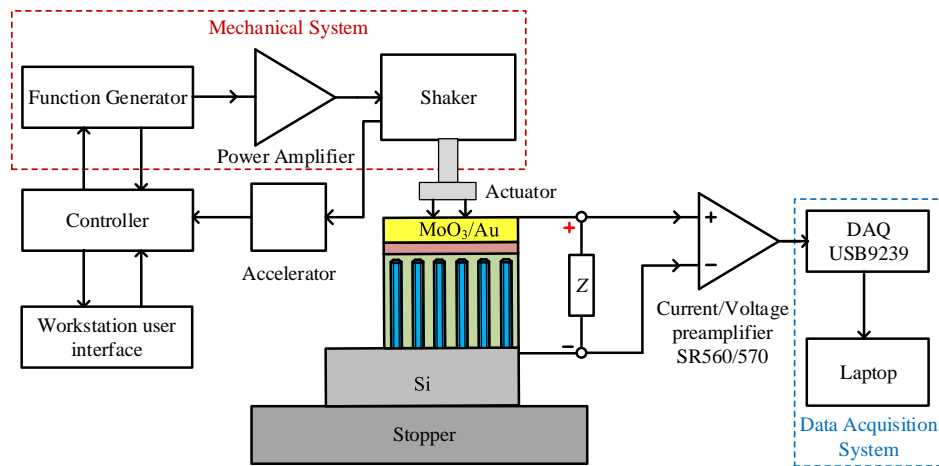


**Fig. S5** The schematic setup for measuring the output current/voltage of fabricated InN NW-based NGs. The system includes a close loop controller (Vibration Research Corporation, VR9500) and a linear shaker (Labworks Inc., ET-126B-1). The shaker provides sinusoidal waves simulating a vibration source with a known amplitude. Output voltage and current signals are measured using Stanford low-noise voltage/current preamplifiers (Model SR560/570) and a National Instruments I/O module (NI CompactDAQ USB-9239). The input resistances of the preamplifiers are 100 M $\Omega$  (SR560) and 10 k $\Omega$  (SR570), respectively.

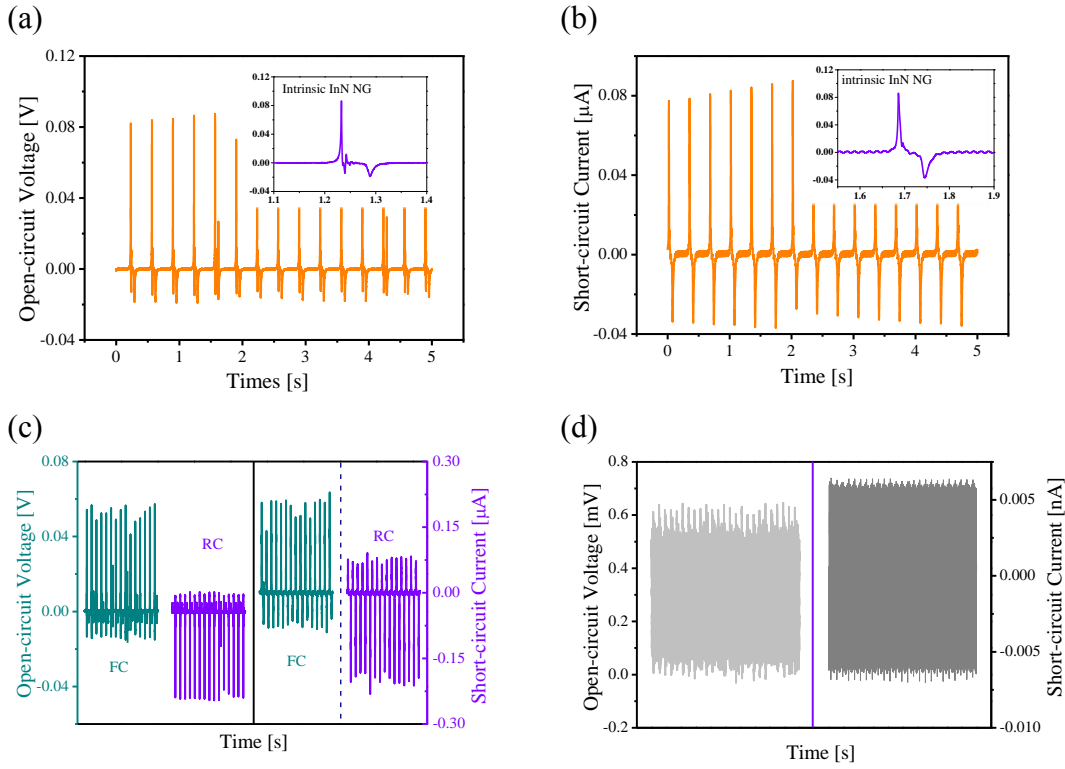


**Fig. S6** The piezoelectric characteristics of the NGs at an excitation with an acceleration amplitude of  $2 \text{ m/s}^2$  and a frequency of 3 Hz. The measured (a) open-circuit voltage, an average peak value of  $\sim 0.085 \text{ V}$ , and (b) short-circuit current, an average peak value of  $80 \text{ nA}$ , for intrinsic-type. The insets show signals from one cycle of mechanical vibration. (c) The measured open-circuit voltage and short-circuit current of the *p*-type NG under the forward and reversed connection conditions. (d) The measured open-circuit voltage and short-circuit current of the Si/PMMA/MoO<sub>3</sub>/Au film.